Propagation in an elastic wedge using the virtual source technique

Ahmad T. Abawi and Michael B. Porter
Heat, Light, and Sound Research, Inc., San Diego, California 92130

(Received 3 August 2006; revised 4 December 2006; accepted 8 December 2006)

The virtual source technique, which is based on the boundary integral method, provides the means to impose boundary conditions on arbitrarily shaped boundaries by replacing them by a collection of sources whose amplitudes are determined from the boundary conditions. In this paper the virtual source technique is used to model propagation of waves in a range-dependent ocean overlying an elastic bottom with arbitrarily shaped ocean-bottom interface. The method is applied to propagation in an elastic Pekeris waveguide, an acoustic wedge, and an elastic wedge. In the case of propagation in an elastic Pekeris waveguide, the results agree very well with those obtained from the wavenumber integral technique, as they do with the solution of the parabolic equation (PE) technique in the case of propagation in an acoustic wedge. The results for propagation in an elastic wedge qualitatively agree with those obtained from an elastic PE solution. © *2007 Acoustical Society of America.* [DOI: 10.1121/1.2431336]

PACS number(s): 43.30.Ma [AIT] Pages: 1374–1382

I. INTRODUCTION

An exact solution of the wave equation is possible only for a range-independent waveguide with plane parallel boundaries. In this case the wave equation is separable in a curvilinear coordinate system and the solution can be represented rigorously by a wavenumber integral. This solution can also be effectively expressed as a sum of propagating normal modes and a spectral integral representing the continuum. One of the distinct features of propagation in a range-independent waveguide is that, a mode, once excited, propagates without coupling with other modes. This forms the basis of the normal mode technique for the solution of the wave equation in a range-independent waveguide. The separability of the wave equation in a range-independent waveguide lends itself to solutions by a number of other techniques, most notably the wavenumber integration, the normal mode method, and the parabolic equation (PE) method.[1] The normal mode and the wavenumber integration techniques can also rigorously treat propagation of waves in an ocean overlying an elastic bottom.

In a range-dependent ocean environment, where the water depth and/or the ocean parameters vary with range, the wave equation is generally not separable. In this case the description of the solution in terms of previously uncoupled modes introduces mode coupling, as was shown by the coupled mode theory developed by Pierce[2] and Milder.[3] If this coupling is ignored, an adiabatic mode solution is obtained, which is accurate for gently varying water depth. However, adiabatic mode theory is unable to describe the transition of modes from trapped, where they are conventionally defined, through cutoff to the leaky state. Since the original work of Pierce and Milder a number of authors have contributed to this technique.[4–9] The technique is essentially based on expressing the field in a range-dependent waveguide in terms of local modes with range-dependent mode amplitudes. The application of the continuity of pressure and the normal component of particle velocity allows a partial separation of the depth and range variables and yields a system of coupled differential equations for the mode amplitudes. However, recent advances in the parabolic equation technique[10,11] have made it the method of choice for modeling propagation in a range-dependent ocean. The parabolic equation technique provides a one-way solution to the wave equation by factoring the range operator into outgoing and incoming operators and ignoring the factor, which contains the incoming operator. While this factorization is exact in a range-independent waveguide, it is an approximation in a range-dependent waveguide and only valid for small bottom slopes.

In most ocean acoustic applications the ocean bottom is modeled as a fluid. Modeling the ocean bottom as an elastic medium presents a number of problems in range-dependent modeling. In the case of the parabolic equation, there is not a clear choice of the dependent variable for which a parabolic equation can be derived. For some choices, the range operator cannot be factored and for some other choices the variables are not continuous across the interfaces, which causes numerical difficulties. Similarly, even though coupled mode solutions for a fluid overlying an elastic bottom have been formulated,[12,13] computation of modes in the vicinity of the region where they transition from trapped to leaky presents numerical difficulties. These difficulties arise mainly because there is no obvious way to keep track of a mode's identity as it goes through cutoff, resulting in misinterpreting the exchange of energy between a set of modes and causing discontinuities to appear in the values of the computed field quantities.

In this paper we use the method of virtual sources to compute propagation in a range-dependent waveguide. This method has widely been used in target scattering computations, particularly when the target is located in a waveguide,[14–17] but its use in modeling propagation in a waveguide is relatively recent.[18] The method is based on

 0001-4966/2007/121(3)/1374/9/$23.00

modeling a boundary or an interface by a collection of sources with unknown complex amplitudes. The functions representing the sources must satisfy the wave equation and the radiation condition in the far field. The amplitudes of the sources are determined in a manner by which the field produced by them and the incident field satisfy all the required boundary and interface conditions. This, in principle, provides an exact solution of the wave equation in a waveguide of arbitrary cross section. The accuracy of the solution is a function of the number of sources, and in most cases the use of five to ten sources per wavelength produces sufficiently accurate results. The sources are usually placed a fraction of a wavelength from a contour following the boundary. The formulation presented in this paper is specific to a waveguide composed of an isovelocity water layer over an acoustic or elastic half-space bottom. However, the water depth can be an arbitrary function of range. The case of a waveguide with a variable sound speed profile overlying a bottom composed of multiple layers will be addressed in a future paper. Even though the technique does not place any restrictions on the shape of the boundary, we apply this technique to a penetrable oceanic wedge. The reason we have chosen the wedge is that it has a simple geometry yet it possesses most of the interesting physical properties of a range-dependent waveguide. Furthermore, the wedge has been studied by numerous authors,[19–22] whose works provide valuable benchmark solutions. The main purpose of this paper is to provide a benchmark solution for an oceanic wedge of arbitrary bottom slope overlying a fluid bottom or an elastic bottom (henceforth referred to as an acoustic or an elastic wedge, respectively). For simplicity of presentation, we model a wedge in a two-dimensional ocean, realizing that modification to a three-dimensional ocean is straightforward. We will, however, discuss the use of the virtual source technique in modeling propagation in an azimuthally symmetric ocean in Appendix A.

This paper is organized as follows: In Sec. II propagation in range-dependent waveguide is formulated for an isovelocity fluid layer overlying an isovelocity fluid or elastic half space. In Sec. III the method is applied to an acoustic and elastic Pekeris waveguide and to an acoustic and an elastic wedge and the results are compared to available published results. The paper concludes with a discussion in Sec. IV.

II. FORMULATION

A. The acoustic case

This formulation is carried out in a two-dimensional Cartesian coordinate system (x,z). The z axis is pointing downward and the plane $z=0$ represents the ocean surface. The Helmholtz equation for a line source at (x',z') is given by

$$\left[\frac{\partial^2}{\partial x^2}+\frac{\partial^2}{\partial z^2}+k^2\right]G_p(\mathbf{r},\mathbf{r}')=\delta(x-x')\delta(z-z'), \tag{1}$$

where

$$\mathbf{r}=(x,z), \quad \mathbf{r}'=(x',z').$$

The Green's function, $G_p(\mathbf{r},\mathbf{r}')$ is given by

$$G_p(\mathbf{r},\mathbf{r}')=\frac{i}{4}H_0^{(1)}(k|\mathbf{r}-\mathbf{r}'|), \tag{2}$$

where the subscript p is used to indicate that G_p is a pressure Green's function. Later we will also introduce G_u, the displacement Green's function. The Green's function given by Eq. (2) is a fundamental solution of Eq. (1) and satisfies the Sommerfeld radiation condition in the far field. These two conditions make $G(\mathbf{r},\mathbf{r}')$ suitable for use as basis functions in the virtual source technique.

Let us represent the bottom boundary by $h(x)$ and the unit normal to the boundary by

$$\hat{\mathbf{n}}=\frac{(-\nabla h,1)}{\sqrt{1+(\nabla h)^2}}.$$

We intend to solve the Helmholtz equation for the pressure $p(x,z)$,

$$[\nabla^2+k^2]p(x,z)=0, \tag{3}$$

for the following boundary conditions:

$$p(x,0)=0,$$

$$[p]_-^+=0, \quad [\hat{\mathbf{n}}\cdot\mathbf{u}]_-^+=0. \tag{4}$$

The above equations express the pressure-release boundary condition at the ocean surface and the continuity of pressure and normal displacement at the water-bottom interface. Since the basis functions given by Eq. (2) satisfy Eq. (3), they will be used by the virtual source technique to express the solution as a sum of basis functions. The boundary conditions given by Eq. (4) will subsequently be imposed. Since two sets of boundary conditions need to be satisfied at the interface, two sets of virtual sources are needed. To do this, a set of sources is placed just below the interface to produce the field in water and another set of sources is placed just above the interface to produce the field in the bottom. Let N denote the number of sources, and let the position of source i be denoted by the position vector $r_i=(x_i,z_i)$. Let $\mathbf{r_1}$ represent the location of the sources that produce the field in the water and $\mathbf{r_2}$ represent the location of the sources that produce the field in the bottom. Let us also represent by $\mathbf{r_a}$ the location of points on the interface or nodes where the boundary conditions will be imposed. The pressure-release boundary condition at the flat ocean surface can be constructed by the method of images. Therefore, the Green's function for the field in the water produced by the sources located at $\mathbf{r_p}$ is

$$\mathbf{G_p}^{(1)}(\mathbf{r};\mathbf{r_1})=\frac{i}{4}\mathbf{H}_0{}^{(1)}(k_1|\mathbf{r}-\mathbf{r_1}|)-\frac{i}{4}\mathbf{H_0}^{(1)}(k_1|\mathbf{r}-\mathbf{r_1^i}|),$$

where $\mathbf{r_1^i}$ represents the location of the image sources. In the above equation all the quantities represented by capitol bold letters are matrices. For example, the entries of $\mathbf{H_0^{(1)}}(k_1|\mathbf{r}-\mathbf{r}'|)$ are $H_0^{(1)}(k_1|r_i-r_j'|)$, where r, is the location of receiver i and r_j' is the location of source j. In this paper we have adopted the convention of representing vectors by lower-case bold letters and matrices by upper-case bold letters. The Green's function for the field in the bottom produced by the sources located at $\mathbf{r_q}$ is

$$\mathbf{G_p}^{(2)}(\mathbf{r};\mathbf{r_2}) = \frac{i}{4} H_0^{(1)}(k_2|\mathbf{r}-\mathbf{r_2}|).$$

In the above equations $k_1 = \omega/c_w$, $k_2 = \omega/c_b$, where ω is the angular frequency, c_w is the water sound speed and c_b is the bottom sound speed, the subscripts 1 and 2 specify the water and bottom layers, and the position vector $\mathbf{r}$ represents the location of the field points and has the same dimension as $\mathbf{r}_1$ and $\mathbf{r}_2$. Note that the Green's functions in the water automatically satisfies the pressure-release boundary condition at the water surface, $z=0$. The field due to the virtual sources of amplitude $s_1, s_2, \ldots, s_N$ located at $r_1', r_2', \ldots, r_N'$ at a field point r can be written

$$p(r) = \sum_{j=1}^{N} G_p(r;r_j') s_j.$$

In vector notation, this can be expressed as

$$p(r) = \mathbf{G_p}(r;\mathbf{r}')\mathbf{s},$$

and for a vector of field points $r_1, r_2, \ldots, r_N$, vector-matrix notation may be used to write

$$\mathbf{p}(\mathbf{r}) = \mathbf{G_p}(\mathbf{r};\mathbf{r}')\mathbf{s},$$

where in the above $\mathbf{p}$ and $\mathbf{s}$ are column vectors of length N and $\mathbf{G_p}$ is a $N \times N$ matrix. Using the same notation, the field in the water and in the bottom can be expressed as a sum of virtual sources of source amplitude $\mathbf{s_1}$ and $\mathbf{s_2}$,

$$\mathbf{p}^{(1,2)}(\mathbf{r}) = \mathbf{G_p}^{(1,2)}(\mathbf{r};\mathbf{r_{1,2}})\mathbf{s_{1,2}},$$

$$\mathbf{u}^{(1,2)}(\mathbf{r}) = \mathbf{G_u}^{(1,2)}(\mathbf{r};\mathbf{r_{1,2}})\mathbf{s_{1,2}}. \tag{5}$$

where the normal displacement, $\mathbf{u}$, is a column vector whose elements are $u_i = \hat{\mathbf{n}} \cdot \nabla p_i/(\rho\omega^2)$ and $\mathbf{G_u}$ is a matrix whose elements are $G_{u(i,j)} = \hat{\mathbf{n}} \cdot \nabla G_{p(i,j)}/(\rho\omega^2)$. Applying the continuity of pressure and normal displacement at the nodes $\mathbf{r_a}$ gives

$$\mathbf{p}_{inc}(\mathbf{r_a}) + \mathbf{G_p}^{(1)}(\mathbf{r_a};\mathbf{r_1})\mathbf{s_1} = \mathbf{G_p}^{(2)}(\mathbf{r_a};\mathbf{r_2})\mathbf{s_2},$$

$$\mathbf{u}_{inc}(\mathbf{r_a}) + \mathbf{G_u}^{(1)}(\mathbf{r_a};\mathbf{r_1})\mathbf{s_1} = \mathbf{G_u}^{(2)}(\mathbf{r_a};\mathbf{r_2})\mathbf{s_2}. \tag{6}$$

In the above equations $\mathbf{p}_{inc}$ is the incident field due to a source in the water and $\mathbf{u}_{inc}$ is a column vector whose elements are $u_{inc(i)} = \hat{\mathbf{n}} \cdot \nabla p_{inc(i)}/(\rho\omega^2)$. The source amplitudes can be obtained from the solution of the above equations,

$$\mathbf{s_1} = (\mathbf{G_p}^{(1)} - \mathbf{K}\mathbf{G_u}^{(1)})^{-1}(\mathbf{K}\mathbf{u}_{inc} - \mathbf{p}_{inc}),$$

$$\mathbf{s_2} = (\mathbf{L}\mathbf{G_u}^{(2)} - \mathbf{G_p}^{(2)})^{-1}(\mathbf{L}\mathbf{u}_{inc} - \mathbf{p}_{inc}), \tag{7}$$

where

$$\mathbf{K} = \mathbf{G_p}^{(2)}(\mathbf{G_u}^{(2)})^{-1} \quad \text{and} \quad \mathbf{L} = \mathbf{G_p}^{(1)}(\mathbf{G_u}^{(1)})^{-1}.$$

The arguments of the functions in Eq. (7) are those in Eq. (6). The source amplitudes determined from Eq. (7) in conjunction with Eq. (5) give the field anywhere in the waveguide.

B. The elastic case

For an elastic bottom, in addition to the pressure-release boundary conditions at the ocean surface, the following boundary conditions at the water-bottom interface must be satisfied:

$$[\hat{\mathbf{n}} \cdot \mathbf{u}]_-^+ = 0,$$

$$\hat{\mathbf{n}} \cdot \boldsymbol{\tau} \cdot \hat{\mathbf{n}} = -p,$$

$$\hat{\mathbf{n}} \times (\boldsymbol{\tau} \cdot \hat{\mathbf{n}}) = 0. \tag{8}$$

The first equation expresses the continuity of normal displacement and the bottom two express the continuity of the normal component of the stress tensor, $\boldsymbol{\tau}$. We express the field in the bottom as a sum of virtual sources

$$\boldsymbol{\phi}^{(2)}(\mathbf{r}) = \mathbf{G}_{\phi}^{(2)}(\mathbf{r};\mathbf{r_2})\mathbf{s_2},$$

$$\boldsymbol{\psi}^{(2)}(\mathbf{r}) = \mathbf{G}_{\psi}^{(2)}(\mathbf{r};\mathbf{r_3})\mathbf{s_3}. \tag{9}$$

In the above equations ϕ and ψ are the scalar and shear potentials, satisfying

$$[\nabla^2 + k_p^2]\phi^{(2)} = 0,$$

$$[\nabla^2 + k_s^2]\psi^{(2)} = 0,$$

where $k_p = \omega/c_p$ and $k_s = \omega/c_s$, and c_p and c_s are the compressional and shear speeds in the bottom, respectively. The position vectors, $\mathbf{r_2}$ and $\mathbf{r_3}$, represent the location of sources producing the compressional and shear fields in the bottom. The compressional and shear potential Green's functions, $G_{\phi}^{(2)}$ and $G_{\psi}^{(2)}$, satisfy

$$[\nabla^2 + k_p^2]\mathbf{G}_{\phi}^{(2)}(\mathbf{r},\mathbf{r}') = \delta(\mathbf{x}-\mathbf{x}')\delta(\mathbf{z}-\mathbf{z}'),$$

$$[\nabla^2 + k_s^2]\mathbf{G}_{\psi}^{(2)}(\mathbf{r},\mathbf{r}') = \delta(\mathbf{x}-\mathbf{x}')\delta(\mathbf{z}-\mathbf{z}'),$$

whose solutions are

$$\mathbf{G}_{\phi}^{(2)}(\mathbf{r},\mathbf{r}') = \frac{i}{4}\mathbf{H}_0^{(1)}(k_p|\mathbf{r}-\mathbf{r}'|),$$

$$\mathbf{G}_{\psi}^{(2)}(\mathbf{r},\mathbf{r}') = \frac{i}{4}\mathbf{H}_0^{(1)}(k_s|\mathbf{r}-\mathbf{r}'|). \tag{10}$$

The displacement vector can be written in terms of two scalar potentials,

$$\mathbf{u} = \nabla\phi + \nabla \times (0,\psi,0),$$

and the stress tensor in the bottom are related to the displacement according to

$$\boldsymbol{\tau}_{ij} = \lambda\delta_{ij}\left(\frac{\partial \mathbf{u}_1}{\partial x_1} + \frac{\partial \mathbf{u}_2}{\partial x_2} + \frac{\partial \mathbf{u}_3}{\partial x_3}\right) + \mu\left(\frac{\partial \mathbf{u}_i}{\partial x_j} + \frac{\partial \mathbf{u}_j}{\partial x_i}\right).$$

In the above δ_{ij} is the Kronecker delta function and λ and μ are the Lamé constants,

$$\lambda = \rho(c_p^2 - 2c_s^2), \quad \mu = \rho c_s^2.$$

Note that in the above equations the arguments of the components of the fields, $\mathbf{r}$, have been suppressed; instead they

have been expressed using bold face character to indicate that they are vectors.

In two dimensions the components of the stress tensor can be written in terms of the displacement vector as

$$\boldsymbol{\tau}_{xx} = (\lambda + 2\mu)\frac{\partial \mathbf{u}_x^{(2)}}{\partial x} + \lambda \frac{\partial \mathbf{u}_z^{(2)}}{\partial z},$$

$$\boldsymbol{\tau}_{xz} = \mu\left(\frac{\partial \mathbf{u}_x^{(2)}}{\partial z} + \frac{\partial \mathbf{u}_z^{(2)}}{\partial z}\right),$$

$$\boldsymbol{\tau}_{zz} = (\lambda + 2\mu)\frac{\partial \mathbf{u}_z^{(2)}}{\partial z} + \lambda \frac{\partial \mathbf{u}_x^{(2)}}{\partial x},$$

and the displacement vector can be expressed in terms of the potentials

$$\mathbf{u}_x^{(2)} = \frac{\partial \boldsymbol{\phi}^{(2)}}{\partial x} - \frac{\partial \boldsymbol{\psi}^{(2)}}{\partial z}, \quad \mathbf{u}_z^{(2)} = \frac{\partial \boldsymbol{\phi}^{(2)}}{\partial z} + \frac{\partial \boldsymbol{\psi}^{(2)}}{\partial x}.$$

To express the field at points $(\mathbf{r})$ due to sources located at $(\mathbf{r}')$, Eqs. (9) are used, which results in

$$\mathbf{u}_z^{(1)} = \mathbf{E}_z \mathbf{s_1}, \quad \mathbf{u}_x^{(1)} = \mathbf{E}_x \mathbf{s_1},$$

$$\mathbf{u}_z^{(2)} = \mathbf{U}_{z_1} \mathbf{s_2} + \mathbf{U}_{z_2} \mathbf{s_3},$$

$$\mathbf{u}_x^{(2)} = \mathbf{U}_{x_1} \mathbf{s_2} + \mathbf{U}_{x_2} \mathbf{s_3},$$

where

$$\mathbf{E}_z = \frac{1}{\rho_1 \omega^2}\frac{\partial \mathbf{G}_{\mathbf{p}}^{(1)}}{\partial z}, \quad \mathbf{E}_x = \frac{1}{\rho_1 \omega^2}\frac{\partial \mathbf{G}_{\mathbf{p}}^{(1)}}{\partial x},$$

$$\mathbf{U}_{z_1} = \frac{\partial \mathbf{G}_{\phi}^{(2)}}{\partial z}, \quad \mathbf{U}_{z_2} = \frac{\partial \mathbf{G}_{\psi}^{(2)}}{\partial x},$$

$$\mathbf{U}_{x_1} = \frac{\partial \mathbf{G}_{\phi}^{(2)}}{\partial x}, \quad \mathbf{U}_{x_2} = -\frac{\partial \mathbf{G}_{\psi}^{(2)}}{\partial z}.$$

Similarly,

$$\boldsymbol{\tau}_{xx} = [(\lambda + 2\mu)\mathbf{U}_{xx_1} + \lambda \mathbf{U}_{zz_1}]\mathbf{s_2} + [(\lambda + 2\mu)\mathbf{U}_{xx_2} + \lambda \mathbf{U}_{zz_2}]\mathbf{s_3},$$

$$\boldsymbol{\tau}_{xz} = \mu[\mathbf{U}_{xz_1} + \mathbf{U}_{zx_1}]\mathbf{s_2} + \mu[\mathbf{U}_{xz_2} + \mathbf{U}_{zx_2}]\mathbf{s_3},$$

$$\boldsymbol{\tau}_{zz} = [(\lambda + 2\mu)\mathbf{U}_{zz_1} + \lambda \mathbf{U}_{xx_1}]\mathbf{s_2} + [(\lambda + 2\mu)\mathbf{U}_{zz_2} + \lambda \mathbf{U}_{xx_2}]\mathbf{s_3}.$$

In the above,

$$\mathbf{U}_{xx_1} = \frac{\partial^2 \mathbf{G}_{\phi}^{(2)}}{\partial x^2}, \quad \mathbf{U}_{zz_1} = \frac{\partial^2 \mathbf{G}_{\phi}^{(2)}}{\partial z^2},$$

$$\mathbf{U}_{xx_2} = -\frac{\partial^2 \mathbf{G}_{\psi}^{(2)}}{\partial x\, \partial z}, \quad \mathbf{U}_{zz_2} = \frac{\partial^2 \mathbf{G}_{\psi}^{(2)}}{\partial z\, \partial x},$$

$$\mathbf{U}_{xz_1} = -\frac{\partial^2 \mathbf{G}_{\phi}^{(2)}}{\partial x\, \partial z}, \quad \mathbf{U}_{zx_1} = \mathbf{U}_{xz_1},$$

$$\mathbf{U}_{xz_2} = -\frac{\partial^2 \mathbf{G}_{\psi}^{(2)}}{\partial z^2}, \quad \mathbf{U}_{zx_2} = \frac{\partial^2 \mathbf{G}_{\psi}^{(2)}}{\partial x^2}.$$

Let us write the unit normal to the interface as

$$\hat{\mathbf{n}} = n_x \hat{\mathbf{x}} + n_z \hat{\mathbf{z}},$$

and further define

$$\mathbf{A}_1 = (\lambda + 2\mu)\mathbf{U}_{xx_1} + \lambda \mathbf{U}_{zz_1},$$

$$\mathbf{A}_2 = (\lambda + 2\mu)\mathbf{U}_{xx_2} + \lambda \mathbf{U}_{zz_2},$$

$$\mathbf{B}_1 = (\lambda + 2\mu)\mathbf{U}_{zz_1} + \lambda \mathbf{U}_{xx_1},$$

$$\mathbf{B}_2 = (\lambda + 2\mu)\mathbf{U}_{zz_2} + \lambda \mathbf{U}_{xx_2},$$

$$\mathbf{C}_1 = \mathbf{U}_{xz_1} + \mathbf{U}_{zx_1},$$

$$\mathbf{C}_2 = \mathbf{U}_{xz_2} + \mathbf{U}_{zx_2}.$$

The boundary conditions given by Eq. (8) can be written

$$(n_x\, \partial\, \mathbf{p}/\partial_x + n_z\, \partial\, \mathbf{p}/\partial_z)/\rho\omega^2 = n_x \mathbf{u}_x^{(2)} + n_z \mathbf{u}_z^{(2)},$$

$$-\mathbf{p} = n_x^2 \boldsymbol{\tau}_{xx} + n_z^2 \boldsymbol{\tau}_{zz} + 2n_x n_z \boldsymbol{\tau}_{xz},$$

$$(n_x^2 - n_z^2)\boldsymbol{\tau}_{zx} + n_x n_z(\boldsymbol{\tau}_{zz} - \boldsymbol{\tau}_{xx}) = 0.$$

In the above equation $\mathbf{p}$ is the total pressure in the water. Substituting for the pressure, the components of displacement, and the stress tensor in terms of the source amplitudes, we get

$$(n_x\, \partial\, \mathbf{p}_{inc}/\partial_x + n_z\, \partial\, \mathbf{p}_{inc}/\partial_z)/\rho\omega^2 + (n_x \mathbf{E}_x + n_z \mathbf{E}_z)\mathbf{s_1} = (n_x \mathbf{U}_{x_1} + n_z \mathbf{U}_{z_1})\mathbf{s_2} + (n_x \mathbf{U}_{x_2} + n_z \mathbf{U}_{z_2})\mathbf{s_3},$$

$$-\mathbf{p}_{inc} - \mathbf{G}_p^{(1)}\mathbf{s_1} = (n_x^2 \mathbf{A}_1 + n_z^2 \mathbf{B}_1 + 2n_x n_z \mathbf{C}_1)\mathbf{s_2} + (n_x^2 \mathbf{A}_2 + n_z^2 \mathbf{B}_2 + 2n_x n_z \mathbf{C}_2)\mathbf{s_3},$$

$$[(n_x^2 - n_z^2)\mathbf{C}_1 + n_z n_x(\mathbf{B}_1 - \mathbf{A}_1)]\mathbf{s_2} + [(n_x^2 - n_z^2)\mathbf{C}_2 + n_z n_x(\mathbf{B}_2 - \mathbf{A}_2)]\mathbf{s_3} = 0.$$

The above equations can be solved to give

$$\mathbf{s_1} = (-\mathbf{G}_{\mathbf{p}}^{(1)} - \mathbf{K}\mathbf{G}_{\mathbf{u}}^{(1)})^{-1}(\mathbf{K}\mathbf{u}_{inc} + \mathbf{p}_{inc}),$$

$$\mathbf{s_2} = (-\mathbf{L}\tilde{\mathbf{G}}_{\mathbf{u}}^{(2)} - \tilde{\mathbf{G}}_{\mathbf{p}}^{(2)})^{-1}(\mathbf{L}\mathbf{u}_{inc} + \mathbf{p}_{inc}),$$

$$\mathbf{s_3} = -\boldsymbol{\Lambda}_3 \boldsymbol{\Lambda}_2 \mathbf{s_2}, \tag{11}$$

where

$$\boldsymbol{\Lambda}_2 = (n_x^2 - n_z^2)\mathbf{C}_1 + n_z n_x(\mathbf{B}_1 - \mathbf{A}_1),$$

$$\boldsymbol{\Lambda}_3 = (n_x^2 - n_z^2)\mathbf{C}_2 + n_z n_x(\mathbf{B}_2 - \mathbf{A}_2),$$

$$\tilde{\mathbf{G}}_p^{(2)} = \boldsymbol{\Gamma}_2 - \boldsymbol{\Gamma}_3 \boldsymbol{\Lambda}_3^{-1} \boldsymbol{\Lambda}_2,$$

$$\tilde{\mathbf{G}}_u^{(2)} = \boldsymbol{\Upsilon}_2 - \boldsymbol{\Upsilon}_3 \boldsymbol{\Lambda}_3^{-1} \boldsymbol{\Lambda}_2,$$

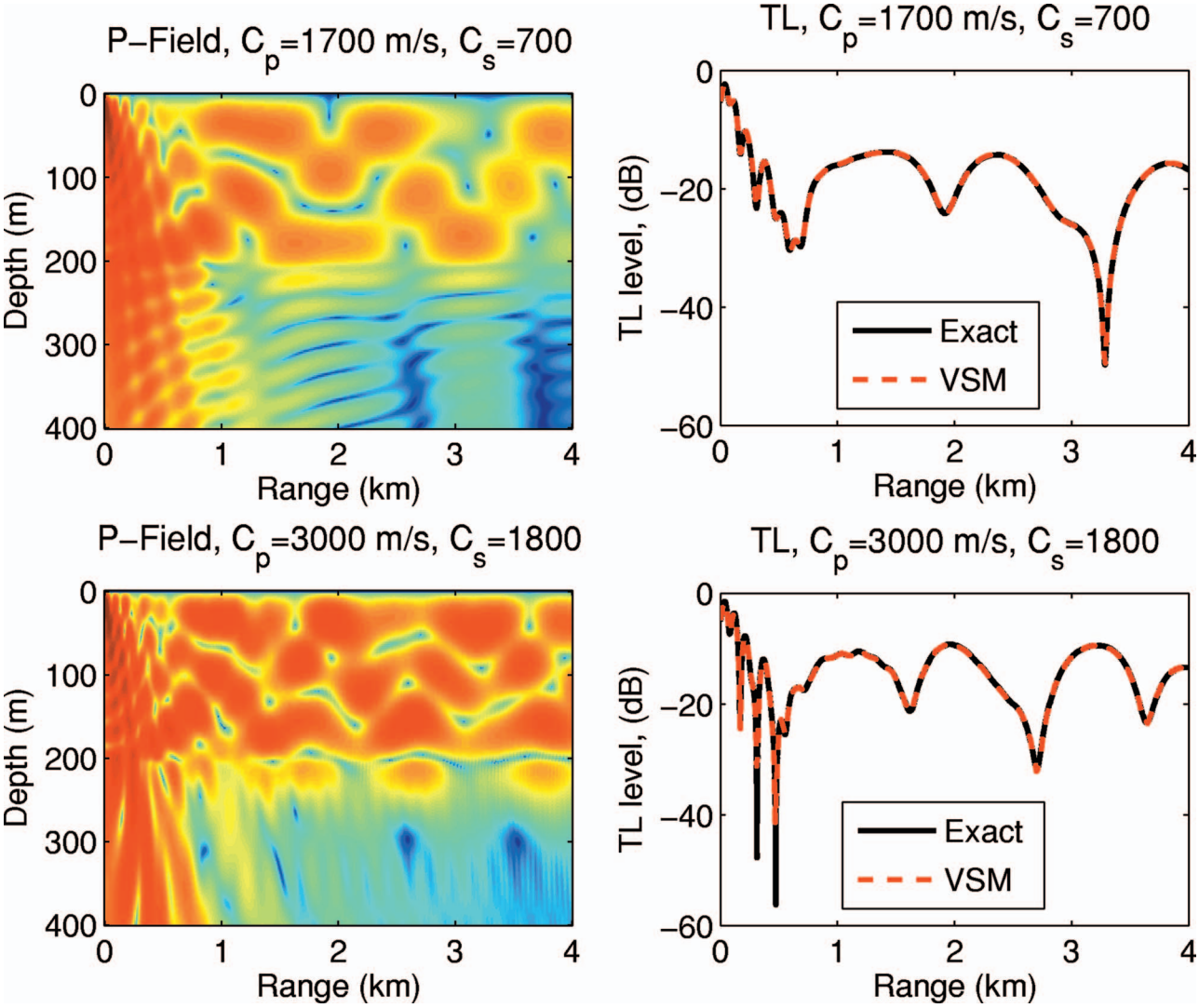

FIG. 1. Propagation in an elastic Pekeris waveguide: The top left panel shows the acoustic field for a 200 m deep water layer over an elastic bottom with compressional sound speed, c_p=1700 m/s, and shear sound speed, c_s=700 m/s. The bottom left panel shows the same for c_p=3000 m/s and c_s=1800 m/s. The right panels show a comparison of transmission loss obtained using the virtual source technique and an exact, wavenumber integration solution. The dynamic range in the field plots is from −60 to 0 dB.

$$\mathbf{\Gamma}_2 = n_x^2\mathbf{A}_1 + n_z^2\mathbf{B}_1 + 2n_x n_z\mathbf{C}_1,$$

$$\mathbf{\Gamma}_3 = n_x^2\mathbf{A}_2 + n_z^2\mathbf{B}_2 + 2n_x n_z\mathbf{C}_2,$$

$$\mathbf{\Upsilon}_2 = n_x\mathbf{U}_{x_1} + n_z\mathbf{U}_{z_1},$$

$$\mathbf{\Upsilon}_3 = n_x\mathbf{U}_{x_2} + n_z\mathbf{U}_{z_2},$$

$$\mathbf{K} = \tilde{\mathbf{G}}_p^{(2)}(\tilde{\mathbf{G}}_u^{(2)})^{-1},$$

$$\mathbf{L} = \mathbf{G}_p^{(1)}(\mathbf{G}_u^{(1)})^{-1}.$$

The source amplitudes given by the above equations completely specify the components of the field anywhere in the waveguide.

III. RESULTS

In this section we apply the model developed in the previous section to various propagation problems. As a first example, we compute the pressure field in a range-independent waveguide composed of an isovelocity water layer over an elastic half-space bottom. Since this problem can be solved exactly by other methods, the purpose of presenting it is to validate the virtual source solution. In this example, a 25-Hz line source is placed at a depth of 30 m. The problem is solved for two sets of bottom paramters. In case 1 the bottom compressional sound speed c_p =1700 m/s and its shear sound speed c_s=700 m/s; in case 2, c_p=3000 m/s and c_s=1800 m/s. In both cases, the bottom compressional attenuation is 0.5 dB/λ and its shear attenuation is 0.25 dB/λ. Attenuation enters the computations through the complex wavenumbers according to $k_{p,s}$ $=\omega/c_{p,s}(1+\lambda_{p,s}/54.58i)$.[23] The results are shown in Fig. 1. The two panels on the left show the compressional pressure field in the waveguide for the two cases and the two panels on the right show transmission loss as a function of range for a receiver at 50 m. The transmission loss obtained from the virtual source technique for the two cases is compared with

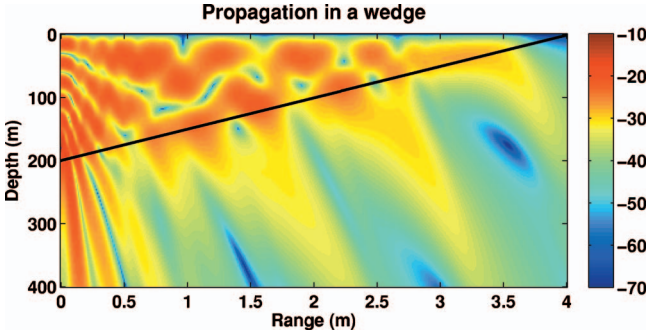

FIG. 2. Propagation in an oceanic wedge using the virtual source technique: In the above figure a 25 Hz source is located at 180 m. The water depth, which is 200 m at the source location, decreases to zero at 4000-m range, resulting in a wedge angle of approximately 2.86 deg. As can be seen, the virtual source technique correctly accounts for mode cutoff.

the exact solution. It should be pointed out that in all examples in this paper we used ten virtual sources per wavelength: It can be seen that the virtual source solutions agree very well with the exact solution. It should be noted that the virtual source technique is designed to force boundary conditions at an arbitrarily shaped boundary or interface. In this example, the method is validated for a simple boundary only because it offers an exact solution. However, this validation confirms that the method is based on sound foundations and gives reason to believe that it can produce equally accurate results for more complicated boundaries. The exact solution, which is used in the validation, will be described in Appendix B.

As a second example, we apply the model to propagation in an oceanic wedge. The wedge is modeled exactly as the ASA Benchmark problem.[24] It is composed of a water layer over an acoustic (no shear) half-space bottom. The water depth decreases as a function of range from 200 m at zero range to 0 at 4000 m range, resulting in a wedge angle of approximately 2.86 deg. The source is a 25-Hz line source, the bottom sound speed is 1700 m/s, and its attenuation is 0.5 dB/λ. The acoustic field in the wedge is shown in Fig. 2. The black line in Fig. 2 indicates the water/bottom interface. As the water depth decreases as a function of range, the three propagating modes cut off one after the other. As can be seen in the figure, the model correctly accounts for this process. Figure 3 shows a comparison of transmission loss for two receiver depths, 100 and 150 m, computed using our model and the parabolic equation (PE) model for a line source. The source in both cases was at 100 m. The small differences between the virtual source solution and the PE solution may be associated with the fact that the PE solution is one-way, accurate within the accuracy of the paraxial approximation, where the virtual source solution is an exact solution.

As a final example, we computed the compressional and shear potentials for an elastic wedge. The results are shown in Figs. 4 and 5. In Fig. 4 the bottom compressional sound speed c_p=1700 m/s and its shear sound speed c_s=700 m/s. The top panel shows the compressional potential field and the bottom panel shows the shear potential field for a 25-Hz source located at 180 m. Figure 5 shows the same for the case when c_p=3000 m/s and c_s=1800 m/s. The results for this example compare well with those obtained using the parabolic equation method in Fig. 3 of Ref. 25. The source distribution for this example is shown in Fig. 6.

IV. SUMMARY

Boundary integral methods essentially take advantage of the divergence theorem to replace a partial differential equation in a volume with an integral equation along a boundary, with the free-space Green's function expressing how points on the boundary mutually affect each other. The virtual source method is really just a boundary integral method that emphasizes the view of points on the boundary as discrete sources and receivers.

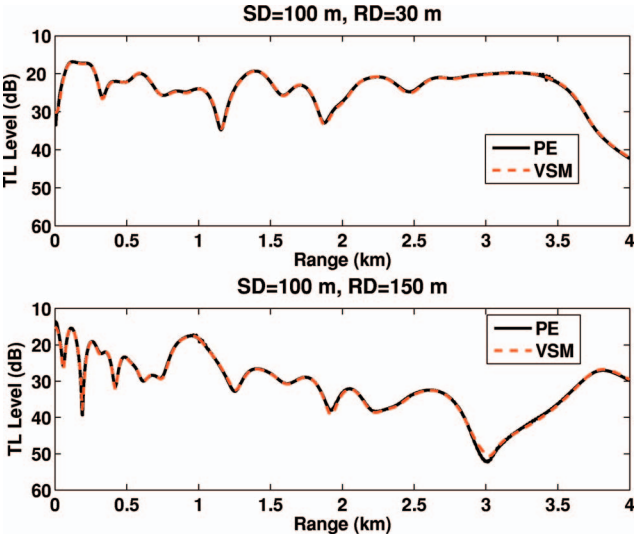

FIG. 3. The above figure shows a comparison of transmission loss obtained using the virtual source technique and the parabolic equation (PE) in an oceanic wedge. The line source is located at 100 m. The receiver in the top figure is at 30 m and in the bottom figure is at 150 m.

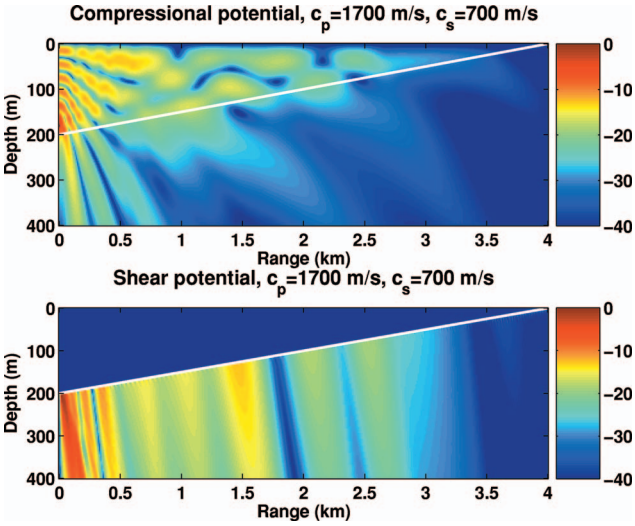

FIG. 4. The above figure shows the compressional and shear potentials in an elastic wedge in the case where the compressional sound speed c_p =1700 m/s and the shear sound speed c_s=700 m/s in the bottom. A 25 Hz source is located at 180 m and the compressional and shear attenuation are 0.5 dB/λ and 0.25 dB/λ, respectively.

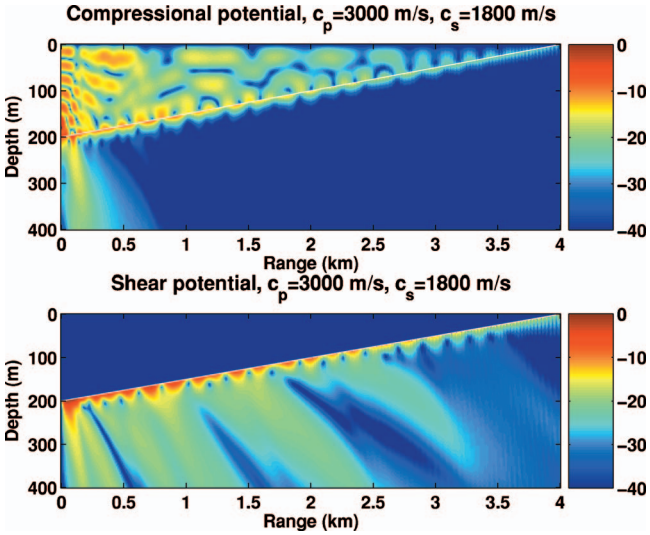

FIG. 5. The above figure shows the compressional and shear potentials in an elastic wedge in the case where the compressional sound speed c_p =3000 m/s and the shear sound speed c_s=1800 m/s in the bottom. A 25-Hz source is located at 180 m and the compressional and shear attenuation are 0.5 dB/λ and 0.25 dB/λ, respectively. These results compare well with those obtained using the PE method in Fig. 3 of Ref. 25.

To date, the virtual source method has been used principally for target scattering problems in ocean waveguides—the target then provides a natural boundary. However, the method has much broader applicability. The work of Fawcett[18] for a rough surface patch provides an important example of that. In this paper we have shown that the method can be used for complicated elastic range-dependent waveguides, providing an essentially exact solution. The application to elastic problems is particularly important in providing benchmark-quality solutions for other emerging methods for elastic problems based on the parabolic equation, finite elements, and coupled modes. While simple geometries, such as the wedge, have been shown here, we emphasize that the method is not restricted to flat boundaries. Further, problems with sound-speed gradients may be handled by substituting the appropriate Green's function, which in turn may be computed in various ways. This latter generalization will be the subject of a future paper.

ACKNOWLEDGMENTS

This work was supported by the Office of Naval Research. The authors would like to thank the reviewers for their thorough evaluation of this paper and their constructive comments.

APPENDIX A: THE VIRTUAL SOURCE TECHNIQUE IN AN AZIMUTHALLY SYMMETRIC OCEAN

In an azimuthally symmetric ocean any source not located at the origin is a ring source centered at the origin. To derive the Green's function for a ring source of source strength S_w in free space, consider the wave equation

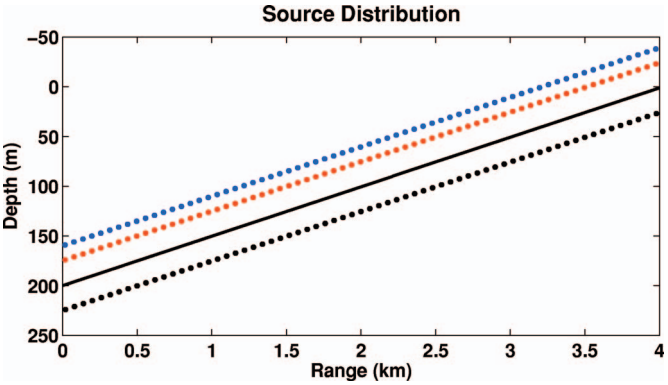

FIG. 6. This figure shows the source distribution for the example of propagation in an elastic wedge. To be able to see the sources, only one in every ten have been shown. The solid line shows the water/bottom interface. The sources represented by the black dots are those that produce the field in the water and those represented by the red and the blue dots are the ones that produce the compressional and the shear potentials in the bottom, respectively.

$$[\nabla^2 + k^2]\psi(r,z) = S_w \delta(z - z_s)\frac{\delta(r - r_s)}{2\pi r}. \tag{A1}$$

Performing the forward Hankel transform,

$$f(k_r,z) = \int_0^\infty \tilde{f}(r,z) J_0(k_r r) r\, dr,$$

on the above equation gives

$$\left(\frac{d^2}{dz^2} + k_z^2\right)\tilde{\psi}(k_r,z) = \frac{S_w}{2\pi}\delta(z - z_s)J_0(k_r r_s),$$

where $k_z^2=(k^2-k_r^2)$. The solution of the above equation is given by[26]

$$\tilde{\psi}(k_r,z) = -S_w J_0(k_r r_s)\frac{e^{ik_z|z-z_s|}}{4\pi i k_z}. \tag{A2}$$

By performing the inverse Hankel transform on Eq. (A2), the Green's function for a ring source in an azimuthally symmetric ocean can be obtained:

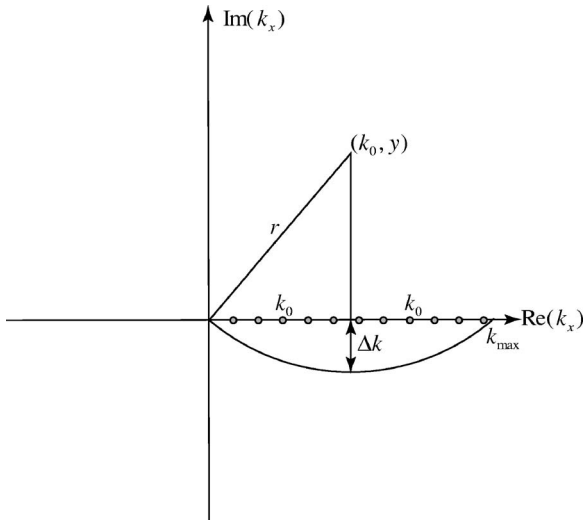

FIG. 7. The arc contour used in the integration of Eq. (B2).

$$G(r,z;r_s,z_s) = -\frac{S_w}{4\pi i}\int_0^\infty \frac{e^{ik_z|z-z_s|}}{k_z} J_0(k_r r) J_0(k_r r_s) k_r \, dk_r. \tag{A3}$$

To be able to treat propagation for a point source using the virtual source technique in the wedge described in Secs. II A and II B, assuming that the wedge is azimuthally symmetric, the free space Green's function given by Eq. (A3) should be used instead of the free space Green's function for a line source.

APPENDIX B: AN EXACT WAVENUMBER INTEGRAL SOLUTION

Consider a waveguide composed of an isovelocity water layer of depth h over an elastic half space bottom with density ρ_b and compressional and shear sounds speeds c_p and c_s. The spectral components of the potential field for a line source located at $z=z_s$ satisfy the depth-separated wave equation

$$\left[\frac{d^2}{dz^2} + (k^2 - k_x^2)\right]\phi(k_x,z) = S_w \frac{\delta(z-z_s)}{2\pi},$$

where

$$\phi(x,z) = \int_{-\infty}^{\infty} \tilde{\phi}(k_x,x) e^{ik_x x} \, dk_x. \tag{B1}$$

In the spectral domain, the potential in the water due to a source at $z=z_s$ can be written

$$\tilde{\phi}_1(k_x,z) = S_w \frac{e^{ik_{z_1}|z-z_s|}}{4\pi i k_{z_1}} + Ae^{ik_{z_1}z} + Be^{-ik_{z_1}(z-h)}.$$

In the above equation the first term is the contribution due to the source and the second and the third terms are downward and upward propagating waves, with $k_{z_1} = \sqrt{k_1^2 - k_x^2}$, where $k_1 = \omega/c_1$. In the bottom the upward propagating wave must vanish due to the radiation boundary condition at infinity. The compressional and shear potentials thus can be written as

$$\tilde{\phi}_2(k_x,z) = Ce^{ik_{z_2}(z-h)},$$

$$\tilde{\psi}_2(k_x,z) = De^{i\kappa_{z_2}(z-h)},$$

where $k_{z_2} = \sqrt{k_p^2 - k_x^2}$ and $\kappa_{z_2} = \sqrt{k_s^2 - k_x^2}$, with $k_p = \omega/c_p$ and $k_s = \omega/c_s$. The coefficients A, B, C, and D are determined by satisfying the pressure release boundary condition at $z=0$ and by demanding the continuity of the normal and tangential components of the stress tensor and the normal component of the displacement vector at $z=h$. The result is

$$\begin{pmatrix} 1 & e^{ik_{z_1}h} & 0 & 0 \\ e^{ik_{z_1}h} & 1 & -\frac{\rho_b}{\rho_w}\left(1 - 2\frac{k_x^2}{k_s^2}\right) & -2\frac{\rho_b}{\rho_w}\frac{k_x\kappa_{z_2}}{k_s^2} \\ ik_{z_1}e^{ik_{z_1}h} & -ik_{z_1} & -ik_{z_2} & -ik_x \\ 0 & 0 & 2k_x k_{z_2} & (2k_x^2 - k_s^2) \end{pmatrix} \begin{pmatrix} A \\ B \\ C \\ D \end{pmatrix} = \begin{pmatrix} S_w \frac{ie^{ik_{z_1}z_s}}{4\pi k_{z_1}} \\ S_w \frac{ie^{ik_{z_1}|h-z_s|}}{4\pi k_{z_1}} \\ -S_w \frac{ie^{ik_{z_1}|h-z_s|}}{4\pi} \\ 0 \end{pmatrix}.$$

To convert the solution back to the spatial domain, Eq. (B1) is used. However, since the kernel of the integral is even with respect to k_x, Eq. (B1) can be written

$$\phi(x,z) = 2\int_0^{k_{\max}} \tilde{\phi}(k_x,x)\cos(k_x x)\, dk_x, \tag{B2}$$

where $k_{\max}$ is the maximum value of k_x at which the integral is truncated. In this paper, $k_{\max}$ was chosen to be $2k_w$, where $k_w = \omega/c_w$. Since the integrand has poles on the real axis, which correspond to the eigenvalues of the waveguide, we integrated Eq. (B2) along the arc contour shown if Fig. 7. The contour, which is a section of a circle of radius r, centered at (k_0, y), is designed such that its maximum distance from the real axis, Δk, is always equal to the wavenumber sampling, Δk_x. Based on this consideration, the center of the circle, (k_0, y), is given by

$$k_0 = k_{\max}/2,$$

$$y = (k_0^2 - \Delta k_x^2)/2\Delta k_x.$$

The points on the contour satisfy

$$k = k_x + ik_i,$$

where

$$k_i = y - \sqrt{r^2 - (k_0 - k_x)^2}.$$

[1] F. B. Jensen, W. A. Kuperman, M. B. Porter, and H. Schmidt, in *Computational Ocean Acoustics* (AIP, New York, 1994), Chaps. 4–6.

[2] A. D. Pierce, "Extension of the method of normal modes to sound propagation in an almost-stratified medium," J. Acoust. Soc. Am. **37**, 19–27 (1965).

[3] D. M. Milder, "Ray and wave invariants for sofar channel propagation," J. Acoust. Soc. Am. **46**, 1259–1263 (1969).

[4]S. R. Rutherford and K. E. Hawker, "Consistent coupled mode theory of sound propagation for a class of nonseparable problems," J. Acoust. Soc. Am. **70**(2), 554–564 (1981).
[5]J. A. Fawcett, "A derivation of the differential equations of coupled-mode propagation," J. Acoust. Soc. Am. **92**(1), 290–295 (1992).
[6]R. B. Evans, "A coupled mode solution for acoustic propagation in a waveguide with stepwise depth variations of a penetrable bottom," J. Acoust. Soc. Am. **74**(1), 188–195 (1983).
[7]B. E. McDonald, "Bathymetric and volumetric contributions to ocean acoustic mode coupling," J. Acoust. Soc. Am. **100**(1), 219–224 (1996).
[8]A. T. Abawi, W. A. Kuperman, and M. D. Collins, "The coupled mode parabolic equation," J. Acoust. Soc. Am. **102**(1), 233–238 (1997).
[9]A. T. Abawi, "An energy-conserving one-way coupled mode propagation model," J. Acoust. Soc. Am. **111**(1), Pt. 1, 160–167 (2002).
[10]F. D. Tappert, "The parabolic approximation method," in *Wave Propagation and Under water Acoustics*, edited by J. B. Keller and J. S. Papadakis (Springer-Verlag, New York, 1977), pp. 224–281.
[11]M. D. Collins, "A slipt-step padé solution for the parabolic equation method," J. Acoust. Soc. Am. **93**(4), 1736–1742 (1993).
[12]R. I. Odom, "A coupled mode examination of irregular waveguides including the continuum spectrum," Geophys. J. R. Astron. Soc. **86**, 425–453 (1986).
[13]J. Tromp, "A coupled local-mode analysis of surface-wave propagation in a laterally heterogeneous waveguide," Geophys. J. Int. **117**, 153–161 (1994).
[14]P. R. Stepanishen, "A generalized internal source density method for the forward and backward projection of harmonic pressure fields from complex bodies," J. Acoust. Soc. Am. **101**(6), 3270–3277 (1997).
[15]G. H. Koopman, L. Song, and J. B. Fahnline, "A method for computing acoustic fields based on the principle of wave superposition," J. Acoust. Soc. Am. **86**(6), 2433–2438 (1989).
[16]J. B. Fahnline and G. H. Koopman, "A numerical solution for the general radiation problem based on the combined methods of superposition and singular-value decomposition," J. Acoust. Soc. Am. **90**(5), 2808–2819 (1991).
[17]M. Ochmann, "The source simulation technique for acoustic radiation problems," Acustica **81**, 512–527 (1995).
[18]J. A. Fawcett, "A scattering-chamber approach for solving finite rough surface scattering problems," J. Acoust. Soc. Am. **118**(3), 1348–1357 (2005).
[19]F. B. Jensen and W. A. Kuperman, "Sound propagation in a wedge shaped ocean with penetrable bottom," J. Acoust. Soc. Am. **67**, 1564–1566 (1980).
[20]A. B. Coppens and J. V. Sanders, "Transmission of sound into a fast fluid bottom from an overlaying fluid wedge," in *Proceedings of Workshop on Seismic Propagation in Shallow Water* (Office of Naval Research, Arlington, VA, 1978).
[21]J. M. Arnold and L. B. Felsen, "Rays and local modes in a wedge-shaped ocean," J. Acoust. Soc. Am. **73**(4), 1105–1118 (1983).
[22]J. M. Arnold and L. B. Felsen, "Coupled mode theory of intrinsic modes in a wedge," J. Acoust. Soc. Am. **79**(1), 31–40 (1986).
[23]F. B. Jensen, W. A. Kuperman, M. B. Porter, and H. Schmidt, in *Computational Ocean Acoustics* (AIP, New York, 1994), Chap. 1.
[24]F. B. Jensen and C. M. Ferla, "Numerical solution of range-dependent benchmark problems in ocean acoustica," J. Acoust. Soc. Am. **87**(4), 1499–1510 (1990).
[25]M. D. Collins, "An energy-conserving parabolic equation for elastic media," J. Acoust. Soc. Am. **94**(2), Pt. 1, 975–982 (1993).
[26]F. B. Jensen, W. A. Kuperman, M. B. Porter, and H. Schmidt, in *Computational Ocean Acoustics* (AIP, New York, 1994), Chap. 4.